

Surface Roughness Prediction of EN8 components using deep learning neural network

Ghanshyam Patel^a and M.B.Kiran^a

^aDepartment of Mechanical Engineering,School of Technology,Pandit Deendayal Energy University

ABSTRACT

EN8 is widely used in die making industry. The surface roughness of the die, while machining on EDM (Electric Discharge Machining) depends upon the process parameters of the machine [1]. The evaluation of surface roughness has gained a lot of significance because of its ability to assess the functionality of a component. Knowing surface roughness makes it possible to predict whether a component will succeed or fail when put into service. This has motivated several researchers to work on predicting or measuring surface roughness in the past. To predict surface roughness in electrical discharge machining (EDM) of EN8 steel, an artificial neural network (ANN) model is developed. Machining parameters including pulse on time(T_{on}), pulse off time(T_{off}) and peak current(I_p), are considered as input neurons, and the main types of surface roughness parameters, R_a , R_q , R_z , R_p , R_v , are used as output neurons. Experiments are conducted based on Response surface method (RSM). Feedforward neural network models are developed using input layer with 3 neurons ,one hidden layer containing varying neurons, from 3 to 10. Results obtained from two prediction models of RSM and ANN are compared. It was found that ANN model give best results. Four different training algorithms- are compared to select the best are the Levenberg-Marquardt(LM), Gradient Descent (GD), Gradient Descent Ascent(GDA), Root Mean Square Prop (RP). The best network is selected based on minimum mean squared error (MSE), minimum Mean Absolute Percentage Error (MAPE) and the highest coefficient determination (R^2). Network trained with LM algorithm is found to be the best ANN model to predict surface roughness parameters such as, R_a , R_q and R_v and GD algorithim is best for R_z and R_p . Using separate testing set, the network is also tested and it is observed that the experimental and predicted values are in proximity to each other.

KEYWORDS

Roughness measurement, Response surface method (RSM), Electrical discharge machining (EDM),Roughness prediction, Artificial neural network (ANN)

1. Introduction

Surface roughness is a significant parameter of any machined component. By knowing the surface roughness, it is possible to determine the suitability of the component when it is put into service. Thus, it can be considered an index of the quality of the product. Many aerospace components such as engine piston heads, landing gear etc., are being manufactured by EDM. It is popular because the desired surface finish can be achieved easily, even with hard-to-machine materials. In this machining process, copper or any conductive metal electrode is used as the negative terminal, and the component to be machined is connected to the positive terminal. A very high temper-

ature generates enough spark for enough heat to erode the workpiece component. The dielectric liquid will constantly flush out tiny particles from the machined surface to cool metal pieces and electrodes. It also controls the temperature so that the surface is not damaged. Surface roughness is a vital parameter in all industrial applications including Die making. Since Artificial intelligence's(AI) invention, many researchers have been applying it to many fields, including die making.A popular method for extracting information from unstructured data is the artificial neural network. The extensive connectivity of neurons used in model-based ANN design enhances performance. The input, hidden, and output layers are used by the algorithm presented in this paper. This algorithm determines an initial set of weights and specifies how weights will be applied to improve performance during the training phase. A neuron's reaction to a signal it receives is controlled by an activation function. The sigmoid function is the most frequently utilized. The objective of the current research work is to develop an AI based model to predict surface roughness parameters- R_a , R_q , R_z , R_p , R_v . Earlier attempts by researchers included only prediction of R_a as roughness parameter. Complete characterization of dies require R_q , R_z , R_p , R_v parameters (Table1) as well. In this context the current research work assumes special significance.

Table 1.: Types of Surface Roughness Parameters and its Industrial Applications

| Roughness | Full Name | Industrial Applications |
|------------------|-------------------------------|--|
| Ra | Arithmetic Average Roughness | Quality control in manufacturing, functional performance of components, aesthetics in consumer products. |
| Rq | Root Mean Square Roughness | Tribology studies, friction and wear resistance optimization, surface coating applications. |
| Rz | Maximum Height of the Profile | Functional performance in sealing surfaces, tribology studies, adhesion in surface coatings. |
| Rp | Maximum Peak Height | Friction and wear resistance optimization, adhesive bonding in assembly processes. |
| Rv | Maximum Valley Depth | Friction and wear resistance optimization, adhesive bonding in assembly processes. |

2. Literature survey

Table 2.: A Literature survey

| Year | Author | Process | Material | Input parameter | Objective | Technique | Remark |
|----------|-------------------|---------|---------------------------------------|------------------------|---------------|---|---|
| [1]2020 | Anurag Joshi | EDM | EN8 | Ton, Toff, wire feed | Ra | ERR and MRR | Low MRR |
| [2]2016 | M.M. Ahmad | EDM | Titanium grade-2 | Ton, Toff, Ip | Ra | Regression | MRR |
| [3]2013 | Ushasta Aich | EDM | HSS | Ton, Toff,Ip, | MRR | SVM, PSO,FFD | Optimization |
| [4]2021 | Balsubra maniyan | WEDM | Nitinol SMA Alloy | Ton, Toff,Ip, Vs, Ac | Ra | MRR,RSM-CCD | Optimum Condition for MRR,Ra |
| [5]2015 | Milan Kumar | EDM | EN31 | Ip,Vp, Ton, Toff | Ra | LM,SCX,GDX | ANN=99% RSM=98% |
| [6]2020 | Alessandro Giusti | EDM | W300 ASP23 ,STAVAX | Steel | Ra | CNN-LeNet MODEL | Ra Prediction |
| [7]2021 | Ashish Goyal | EDM | Titanium luminide | Ton, Toff, Ip, | Ra | ANOVA | Ra decrease with Toff, increase with Ton,Ip |
| [8]2020 | Naresh | WEDM | NITINOL | Ton, Toff, Vp | Ra | Adaptive neuro-fuzzy(ANFIS),LM | MRR, Ra |
| [9]2016 | Je-Kang Park | N/a | Stone,Wood, Silicon wafer | Surface | Defect detect | CNN, PSO | CNN netter than PSO |
| [10]2009 | K.M.Patel | EDM | f Al ₂ O ₃ /SiC | Ton,Ip, Vg, Duty cycle | Ra | RSM,ANOVA | Ton is dominant for Ra |
| [11]2019 | Dhiren Patel | Milling | Al | Machined | Ra | GLCM,J48, RF, RBF, SVM, GLCM, | RF,ANN 99 % accuracy |
| [12]2012 | Uma,Paturi | WEDM | Inconel 718 | Ip,Ton | Ra | ANN SVM RSM | SVM Better than ANN,RSM GA Opt |
| [13]2019 | R.R.Paul | EDM | Inconel 800 | Ton, Toff,Ip | Ra | Multi objective optimization & ratio analysis | Optimization of parameters |

Continued on next page

Table 2 – continued from previous page

| Year | Author | Process | Material | Input parameter | Objective | Technique | Remark |
|----------|-----------------|--------------------|-----------------------|---------------------------------------|----------------|--------------------------------|--|
| [14]2020 | B.C.Routara | EDM | T6-Al7075 | Toff,Ip,Spark Gap | kMRR, WTR, Ra | TOPSIS | MRR higher in Rotary mode |
| [15]2020 | Jamal Saeedi, | EDM | Steel | EDM machining | Ra | CNN,VGG, AlexNet, ResNet | CNN based regression and classifier |
| [16]2014 | Shivanna | EDM | Steel | Ton,Ip | Sa,Sq, etc. | MATLAB | CCD,Confocal microscope |
| [17]2022 | Ranjit Singh | EDM | Cu-SMA | Ip,Ton,TWR | Ra | GA,TELBO | ANOVA Optimization |
| [18]2020 | Mustafa Ulas | WEDM | Al7075 Aluminum alloy | Vp,Ton,WFR | Ra | WDM,SVR | W-ELM results are good |
| [19]2022 | Vinay Vakhria | WEDM | NITINOL | Ton,Toff,Ip | Ra | SinGAN, KNN, Alexnet ,DenseNet | SinGAN is effective |
| [20]2021 | Hatrice Varol , | EDM | Inconel 718 | Ton, Toff, Ip | Ra | ANN, GEP, ANN | better than GEP |
| [21]2020 | Yogesh | WEDM | Aluminum composites | Ton, Toff, Ip | Ra, MRR | Decision tree, Nieve Byes | MRR |
| [22]2023 | Zhang | SLM | 316L Stainless steel | Laser power, scanning speed and pitch | Ra | BPNN | No relation between Ra and Rel.Density |
| [23]2021 | Kundark | Turning, Grind-ing | Steel | Feed, DOC, Speed | 2D,3D analysis | Rs, Rq, Rz, Rsk, Rku | Accuracy and Topography |

Table 3.: Abbreviations

| | | |
|---------------------------------|---|---------------------------------|
| EDM: Electric Discharge machine | Ton : Pulse time on | Toff: Pulse time off |
| Ip:Pulsating current | WEDM: Wire Electric Discharge Machining | Ra :Average surface Roughness |
| Vp : Peak Voltage | MRR: Material removal rate | SVR : Support vector Regression |
| ANN : Automatic Neural network | TWR: Tool Wear rate | RSM:Response surface Method |
| ANOVA : Analysis of variance | CCD: Charged couple camera | |

Anurag et al. focus on the EN8 material utilized on the EDM machine in this study performs better than typical mild steel, which has carbon levels between 0.3 and 0.6%. For higher values of the process parameters, the MRR is proportional to the EWR Electrode wear rate [1].

Mustafaiz et al. investigate L18 Orthogonal Array (OA) tests were conducted using input factors such as Peak Current, Duty Cycle, and Voltage Gap. Studies were conducted to determine how machining parameters impacted responses like MRR [2].

Ushasta Aich et al In this study, support vector machines, and PSO are employed to create EDM modeling frameworks. Models for MRR and Ra are created using SVM. To confirm the models' correctness and applicability, testing data sets are used to evaluate them [3].

Balsubramaniam et al.focus the major focus of this study is wire electric discharge machining (W-EDM), which is used in SMA. When analyzing machining parameters, such as surface and material removal, current, servo voltage, and pulse on time were taken into account. pulse-free time. Parametric analysis was completed after the response surface approach-based central composite design [4].

The author investigate an ANN model has been created by the authors to forecast the surface roughness of EN 31 steel. Average roughness (Ra) is the output neuron, whereas machining parameters are the input neurons. A CCD serves to conduct experiments. Based on performance indicators, the best network is chosen after comparing several training techniques. Results from the L-M algorithm are good. When predicting surface roughness, the ANN model outperforms the RSM model. To examine how process variables affect results, 3D surface plots are employed [5].

Allesandro Giusti et al. investigate a Convolutional Neural Network is employed in a cheap optical measurement system that is combined with an EDM machine to forecast Ra values. Experimental results show that predictions made at different roughness levels are accurate. This is an effective method for characterizing and controlling the roughness of surfaces in machining operations [6].

Ashish Goyal et al. use surface roughness optimization on an EDM machine. The Taguchi approach has optimized the results that were achieved. ANOVA analysis reveals important criteria for enhancing surface roughness[7].

Naresh et al focus on Levenberg-Marquardt (LM) algorithms. It was discovered that LM with 10 neurons was the ideal algorithm and number of neurons in the hidden layer for ANN models [8].

Je-Kang Park et al.focus on artificial intelligence (AI) and smart sensors to automatically detect surface flaws in components. The suggested technique uses CNN-based image processing to find wear, scratches, and burrs. The efficiency of a single CNN network for assessing various sorts of flaws on textured and non-textured surfaces was demonstrated through the construction and testing of several neural networks [9].

R.K.Patel et al.;focus on Sorface roughness and EDM machining parameters Ton, Vgap, Duty cycle. Using Response surface Method Ton is found o be dominant parameters[10] .

Dhiren Patel et al. focus on machine learning and image processing techniques are used to identify surface quality from machining surfaces. It offers a technique that uses machine learning algorithms to characterize collected photos by extracting statistical information from them. Results with the ANN and RF algorithms demonstrate remarkable accuracy. This study provides a practical method for evaluating machined surfaces' quality, which is advantageous to sectors including manufacturing and quality control [11].

Uma Maheswari,Reddy Patauri et al. Surface roughness significantly improves by

61.31 when the GA technique is used. These outcomes represent quick and precise WEDM of Inconel 718 prediction and optimization approaches [12].

T. R. Paul et al. investigate the optimization process parameters in Inconel 800 EDM using a hybrid approach. It is very simple to use MOORA, or multi-objective optimization on the basis of ratio analysis, and it is also very simple mathematically.[13].

Routara et al. focus on the EDM machining properties of T6-Al7075. For both rotary and steady tool modes, the parameters Tonne, Toff, Ip, and voltage are used. MRR TWR, Ra, and Rq optimization for responses has been examined [14].

Jamal Seedi et al. investigate the research describes the use of deep neural networks in an industrial measurement system for determining surface roughness and fault detection on degraded steelwork parts. The suggested techniques are superior to others. By combining CNN-based regression with CNN-based classification, we achieve accurate roughness estimation (7.32% error), high defect detection accuracy (97.26%), and precise localization (99.09% area under the ROC curve)[15].

Shivanna et al use this study compares 3D surface roughness metrics using a confocal and CCD camera using aluminum as a specimen metal. The vision approach is a revolutionary technique. [16]. Ranjit Singh et al In this study, EDM settings for a Cu-based shape memory alloy are optimized using machine learning techniques. The study examines how dimensional deviation and tool wear rate are affected by process parameters. The study makes use of a central composite design matrix and employs 2-D and 3-D graphs to illustrate response parameter behavior. Cu-based SMA machining in EDM processes and optimization by Genetic Algorithm, and Teacher Learning-based optimization approaches both involve machine learning [17].

Mustafa Ulas et al.focus on Aluminum alloys are precisely machined using WEDM and can estimate surface roughness, saving time and money compared to experimentation. Al7075 aluminum alloy experiments were conducted with various WEDM parameters, and machine-learning models for surface roughness prediction were built. The model has the accuracy of 0.9720 and has the most potential for use in manufacturing WEDM-produced parts [18] .

Vinay Vakharia et al. focus on Nitinol in manufacturing for biomedical and aeronautical applications is examined in this research. The difficulty of producing desired surface characteristics in machined components is discussed in the paper. FESEM (Electro Microscope) is utilized to analyze the surfaces of Nitinol specimens after wiring electrical discharge machining. Surface morphology and its link to process parameters are predicted using deep learning models, such as SinGAN and DenseNet. A useful tool for surface image prediction in manufacturing, the DenseNet model has great accuracy [19].

Hatice Varol et al use the metal alloy Inconel 718 have excellent mechanical, corrosion-resistance, and high-temperature performance characteristics. However, problems arise from their low machinability and the necessity for expensive tools in conventional machining techniques. For cutting hard materials, non-traditional production techniques like electrical discharge machining offer an affordable solution. An artificial intelligence model for evaluating surface roughness based on process parameters was developed using ANN and GEP[20]. Yogesh et al. draw attention to the difficulties in determining the ideal parameters for the highest MRR and the lowest Ra as well as the limitations of conventional testing techniques. The suggested approach uses Decision Tree and Naive Bayes algorithms to forecast SR and MRR, saving time and important resources. The emphasis is especially on the EDM machining of aluminum composites, demonstrating how the algorithms can be used in this

situation[21].

Zhang et al. focus on selective laser melting (SLM) used back propagation neural networks (BPNN) which quickly predict the surface roughness with high prediction accuracy [22].

Kundrak et al. focus on surface roughness of machined hard material with Ra,Rq,Rz,Rsk,Rku parameter textbf[23].

3. Methodology

The steps mentioned below are used while performing research.

- (1) Specimen preparation.
- (2) Surface roughness measurement .
- (3) Development of model using Artificial Neural Network (ANN).
- (4) Prediction using RSM.
- (5) Prediction using ANN.

3.1. Specimen preparation

Generally, for three parameters and at three levels need 27 (4^3) numbers of experiments to be conducted. Central composite design of experiment suggests very less number of experiments to predict optimized conditions among the assigned parameters with their levels. Taguchi L27 array is found to be suitable for this experimental approach of study. Hence, only 27 experiments are required to be conducted to find the combination of levels of parameters, which give the optimal result. Analysis of Variance (ANOVA) is performed to observe the effects of process parameters. By altering settings during an EDM machining operation, specimens are prepared. In Table 4, I_p , T_{on} , T_{off} are variables and peak Voltage is kept constant When performing an EDM operation on specimens, die electric fluid is employed.



Figure 1.: EDM 27 Nos.specimens on EN8 plate



Figure 2.: EDM machine - Sparkonix

Table 4.: Input parameters

| Design factors | Code | Levels | | |
|-------------------------------------|------|--------|----|----|
| | | -1 | 0 | 1 |
| Pulse on time(T_{on}) μ s | A | 3 | 5 | 7 |
| Pulse off time(T_{off}) μ s | B | 2 | 4 | 6 |
| Discharge Current(I_p)amp | C | 10 | 20 | 30 |

3.2. surface roughness measurement

Surface roughness of the specimens, made with different process parameters, are measured (Table 5) using a profilometer of Mitsubishi model SJ-410 as shown in Figure 3 sets of observations are obtained and the average values are computed for Ra, Rq, Rz, Rp, Rv



Figure 3.: Profilometer-SJ410

Table 5.: Process parameters and Roughness details of Specimens

| No | Ton | Toff | Ip | Ra | Rq | Rz | Rp | Rv |
|----|-----|------|----|-------|-------|--------|--------|--------|
| 1 | 3 | 2 | 10 | 4.252 | 5.585 | 28.935 | 12.071 | 16.865 |
| 2 | 3 | 2 | 20 | 4.442 | 5.664 | 26.886 | 10.423 | 16.462 |
| 3 | 3 | 2 | 30 | 5.428 | 6.928 | 29.213 | 14.856 | 14.356 |
| 4 | 3 | 4 | 10 | 4.317 | 5.309 | 24.604 | 10.612 | 13.992 |
| 5 | 3 | 4 | 20 | 4.489 | 5.518 | 25.57 | 10.429 | 14.141 |
| 6 | 3 | 4 | 30 | 5.061 | 6.529 | 29.292 | 13.338 | 15.954 |
| 7 | 3 | 6 | 10 | 4.047 | 5.047 | 23.099 | 9.117 | 13.982 |
| 8 | 3 | 6 | 20 | 4.372 | 5.399 | 23.959 | 12.019 | 11.94 |
| 9 | 3 | 6 | 30 | 4.681 | 5.705 | 23.789 | 10.131 | 13.658 |
| 10 | 5 | 2 | 10 | 4.296 | 5.735 | 27.909 | 14.507 | 13.402 |
| 11 | 5 | 2 | 20 | 4.706 | 6.136 | 27.858 | 11.558 | 16.3 |
| 12 | 5 | 2 | 30 | 5.077 | 6.45 | 29.005 | 12.618 | 16.388 |
| 13 | 5 | 4 | 10 | 4.506 | 5.695 | 25.707 | 9.887 | 15.82 |
| 14 | 5 | 4 | 20 | 4.761 | 5.803 | 25.066 | 10.824 | 14.242 |
| 15 | 5 | 4 | 30 | 5.561 | 6.807 | 28.956 | 13.056 | 15.9 |
| 16 | 5 | 6 | 10 | 4.742 | 5.915 | 26.665 | 12.601 | 14.064 |
| 17 | 5 | 6 | 20 | 4.864 | 6.344 | 27.857 | 11.205 | 16.651 |
| 18 | 5 | 6 | 30 | 6.48 | 8.296 | 35.502 | 18.892 | 16.61 |
| 19 | 7 | 2 | 10 | 3.936 | 4.971 | 22.736 | 9.606 | 13.13 |
| 20 | 7 | 2 | 20 | 4.278 | 5.611 | 27.583 | 15.535 | 12.048 |
| 21 | 7 | 2 | 30 | 5.007 | 6.013 | 25.309 | 11.77 | 13.539 |
| 22 | 7 | 4 | 10 | 4.133 | 5.202 | 24.117 | 11.084 | 13.033 |
| 23 | 7 | 4 | 20 | 4.389 | 5.409 | 24.965 | 10.593 | 14.372 |
| 24 | 7 | 4 | 30 | 5.177 | 6.337 | 26.83 | 10.833 | 15.997 |
| 25 | 7 | 6 | 10 | 4.746 | 5.719 | 25.865 | 10.565 | 15.3 |
| 26 | 7 | 6 | 20 | 5.016 | 6.19 | 27.16 | 11.631 | 15.53 |
| 27 | 7 | 6 | 30 | 5.274 | 6.357 | 27.608 | 11.603 | 16.004 |

3.3. Development of model using Artificial Neural Network (ANN)

A neural network is made up of a number of layers that each contain various components known as neurons. Network formation determines the network's type. Weights are used in the learning process to convert the network's storage of processing power. The training algorithm is a process that involves changing a network's weights to reduce a chosen function of error between the actual and desired outputs [1]. Today's industrial applications use ANN. ANN can be used in a variety of manufacturing processes. Input, hidden, and output layers make up its three primary layers. The input layer's neurons send information from the outside environment to the hidden layer. Utilizing data from the input layer and the activation, bias, and summation functions, outputs are generated in the hidden layer. The ANN's workings are displayed in Figure 4. The model is developed using Leven Berge-Marqardt algorithm with Adam optimizer. Convolutional Neural Networks (CNNs) are being trained by the authors to analyze and characterize the topology of a surface using the current methodology. The objective is to develop a method that can accurately assess surface topology using CNNs. This machine can generate surfaces with standard characteristics, which are essential for training the CNN models. By producing surfaces with

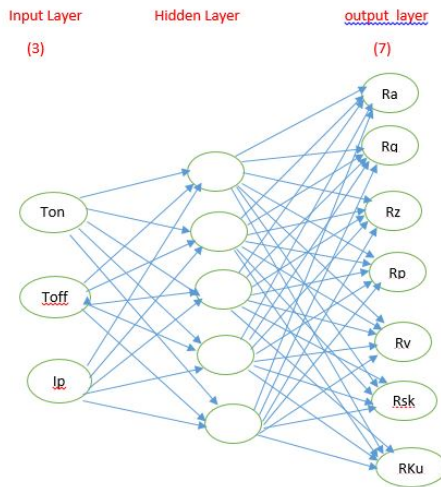


Figure 4.: Neural Network

known characteristics, they can train the CNNs to accurately identify and characterize different surface topologies. The researchers aim to create a robust and versatile system that can analyze and classify surfaces based on their topology, regardless of the specific roughness average (Ra) value. This work has the potential to enhance the understanding and characterization of surfaces in various industries and applications[2]. In the era of rapid development of science and technology, people's requirements for intelligence are getting higher and higher, and artificial intelligence has set off a new wave. Artificial neural networks (ANN) is a computational model that mimics biological neural networks. It evolved from the single-layer perceptron M-P model proposed in 1943 to a computing model that now has a multilayer perceptron network.^{13–16} The computational power is greatly improved and can deal with complex nonlinear problems. It is widely used in model recognition, machine vision, speech recognition, and other artificial intelligence fields. A BP neural network is a feed-forward artificial neural network using an error back propagation algorithm, it has strong adaptive

self-learning ability, superior fault tolerance, and robustness, and is the most widely used of the neural network models. BP neural networks structure is divided into three layers, namely, the input layer, hidden layer, and output layer, through the connection between each layer connection weights and threshold values, as shown in Figure 1. The basic principle is that the input vector flows through the hidden layer and the output layer of the inter-layer transfer function. If the demand is not met, the output value of the neuron is returned. The learning process is modified by modifying the connection weight and threshold value. The whole process continues until the output value meets the requirements and terminates.[22]

The following metrics, defined by equations 1,2 and 3, will be used for testing the efficacy of the prediction model.

Mean Squared Error (MSE):

$$\text{MSE} = \frac{1}{N} \sum_i |t_i - o_i|^2 \quad (1)$$

Mean Absolute Percentage Error (MAPE):

$$\text{MAPE} = \frac{1}{N} \sum_i \left| \frac{t_i - o_i}{t_i} \right| \times 100 \quad (2)$$

R-squared (R^2):

$$R^2 = 1 - \frac{\sum_i (t_i - o_i)^2}{\sum_i (o_i)^2} \quad (3)$$

3.4. Prediction using Response Surface Method(RSM)

Multiple regression is statistical technique to determine predicted values. In order to predict roughness parameters R_a, R_q, R_z, R_p, R_v Equation 4 is used.

$$Y = \beta_0 + \sum_{i=1}^k \beta_i \cdot X_i + \sum_{i=1}^k \beta_{ii} \cdot X_i^2 + \sum_{j>1}^k \beta_{ij} \cdot X_i \cdot X_j + \varepsilon \quad (4)$$

where Y represents the corresponding response, i.e., R_a of EDM process in the present work, X_i is the input variables, X_i^2 and $X_i \cdot X_j$ are the squares and interaction terms, respectively, The influences of EDM parameters (T_{on}, T_{off}, I_p) on surface roughness (R_a) have been assessed for EN8 steel. The second-order model is the relationship between the surface roughness parameter and the Multiple regression is a statistical technique that allows us to determine the correlation between a continuous dependent variable and two or more continuous or discrete independent variables.

Results obtained by using RSM model will be elaborated in section 4.1.

4. Results and Discussion

4.1. ANOVA and regression equation of Ra

ANOVA technique helps in identifying the most influencing factor affecting the output parameter(Ra).The technique uses sum of squares and variance during analysis. Least squares technique is used in this approach. Table 4 shows the input factor levels and input values

Table 6 shows the variance of analysis for Ra.

Table 6.: Variace analysis for Ra

| Source | DF | Adj SS | Adj MS | F-Value | P-Val |
|-----------|----|---------|---------|---------|-------|
| Model | 9 | 6.63904 | 0.73767 | 10.59 | 0 |
| Linear | 3 | 4.75123 | 1.58374 | 22.73 | 0 |
| Ton | 1 | 0.04176 | 0.04176 | 0.6 | 0.449 |
| Toff | 1 | 0.43556 | 0.43556 | 6.25 | 0.023 |
| Ip | 1 | 4.27391 | 4.27391 | 61.34 | 0 |
| Square | 3 | 1.21507 | 0.40502 | 5.81 | 0.006 |
| Ton*Ton | 1 | 0.89218 | 0.89218 | 12.8 | 0.002 |
| Toff*Toff | 1 | 0.01357 | 0.01357 | 0.19 | 0.665 |
| Ip*Ip | 1 | 0.30933 | 0.30933 | 4.44 | 0.05 |
| 2-Way | 3 | 0.67274 | 0.22425 | 3.22 | 0.049 |
| Ton*Toff | 1 | 0.67071 | 0.67071 | 9.63 | 0.006 |
| Ton*Ip | 1 | 0.00066 | 0.00066 | 0.01 | 0.924 |
| Toff*Ip | 1 | 0.00137 | 0.00137 | 0.02 | 0.89 |
| Error | 17 | 1.18447 | 0.06967 | | |
| Total | 26 | 7.82351 | | | |

The surface parameters (R_a) is predicted using input values of T_{on} , T_{off} , I_p

$$\begin{aligned}
 R_a = & 3.27 + 0.744 \cdot T_{on} - 0.302 \cdot T_{off} - 0.0418 \cdot I_p \\
 & - 0.0964 \cdot T_{on}^2 + 0.0119 \cdot T_{off}^2 + 0.00227 \cdot I_p^2 \\
 & + 0.0591 \cdot T_{on} \cdot T_{off} + 0.00037 \cdot T_{on} \cdot I_p - 0.00053 \cdot T_{off} \cdot I_p
 \end{aligned} \tag{5}$$

4.2. RSM surface plots

Figure 5 shows that as value of T_{on} increases R_a is increased but the increase is not significant, whereas it is significant when value of T_{off} is increased

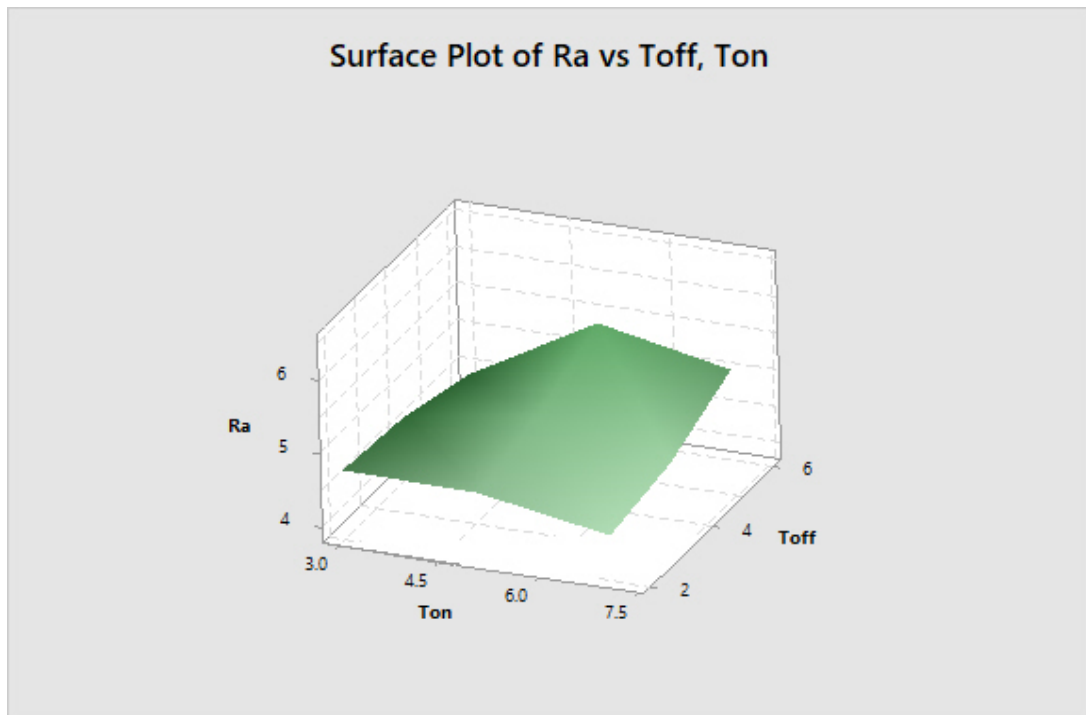


Figure 5.: 3D Plot Ra v/s Toff,Ton

Figure 6 shows that as value of T_{on} increases R_a is increased but the increase is not significant, whereas it is significant when value of I_p is increased

Figure 7 shows that as value of T_{off} increases R_a is not increasing significantly. When value of I_p is increasing R_a is also increasing fast. It indicates that value of peak current affects surface roughness R_a significantly.

Surface Plot of Ra vs Ton, Ip

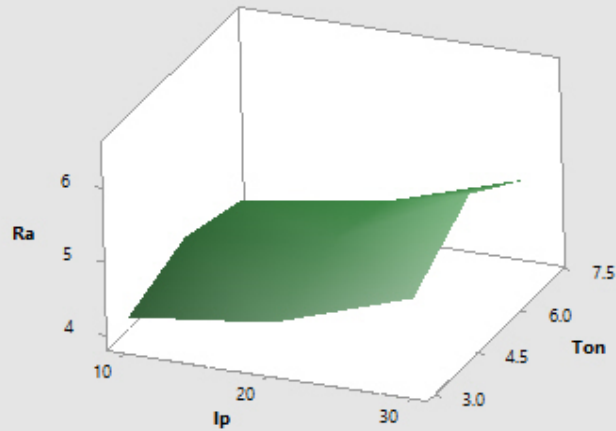


Figure 6.: 3D Plot of Ra v/s Ton, Ip

Surface plot of Ra v/s Toff, Ip

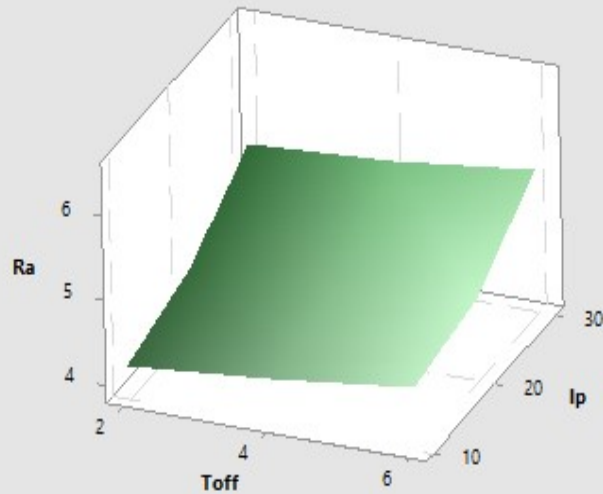


Figure 7.: 3D Plot of Ra v/s Toff, Ip

Figure 8 is bar chart of comparison of actual Ra-values and predicted Ra values. both the values are in proximity, showing strength of RSM model.

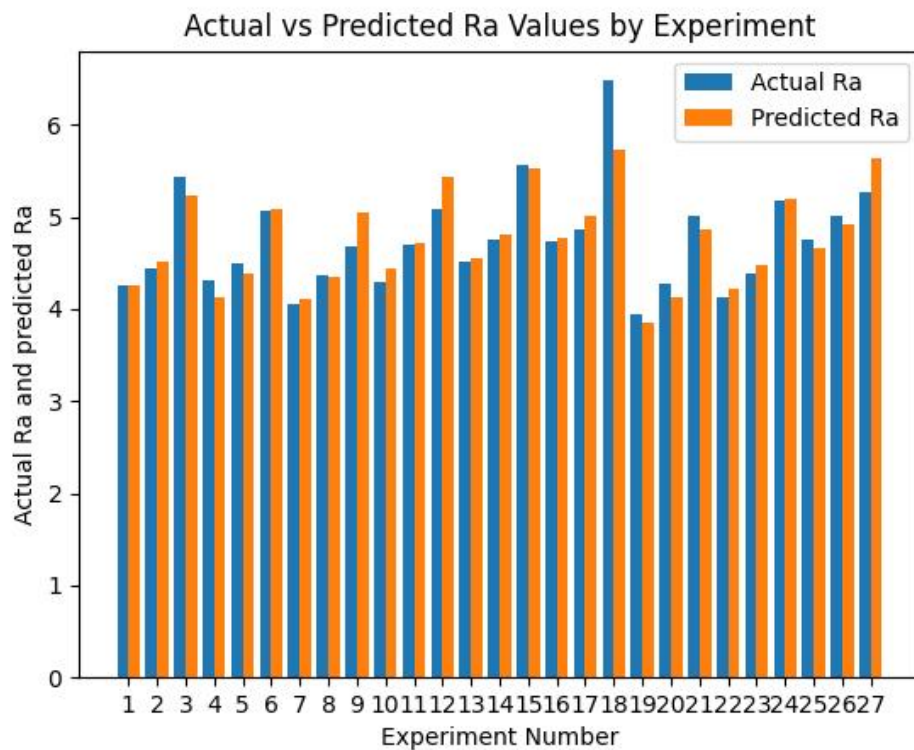


Figure 8.: Comarative graph of RSM for actual and predicted values of surface roughness

Figure ??

4.3. Response surface method (RSM) results

Table 7.: RSM Results

| Exp | Input factors | | | | Experiment Output variables | | | | Predicted output variables | | | | |
|-----|---------------|-----|------|-------|-----------------------------|--------|--------|--------|----------------------------|-------|--------|--------|--------|
| | No | Ton | Toff | Ip | Ra | Rq | Rz | Rp | Rv | pRa | pRq | pRz | pRp |
| 1 | 3 | 2 | 10 | 4.252 | 5.585 | 28.935 | 12.071 | 16.865 | 4.247 | 5.527 | 27.770 | 11.700 | 16.042 |
| 2 | 3 | 2 | 20 | 4.442 | 5.664 | 26.886 | 10.423 | 16.462 | 4.511 | 5.834 | 27.860 | 12.020 | 15.693 |
| 3 | 3 | 2 | 30 | 5.428 | 6.928 | 29.213 | 14.856 | 14.356 | 5.228 | 6.636 | 29.200 | 13.300 | 15.857 |
| 4 | 3 | 4 | 10 | 4.317 | 5.309 | 24.604 | 10.612 | 13.992 | 4.130 | 5.117 | 24.420 | 9.640 | 14.627 |
| 5 | 3 | 4 | 20 | 4.489 | 5.518 | 25.570 | 10.429 | 14.141 | 4.382 | 5.472 | 25.110 | 10.400 | 14.448 |
| 6 | 3 | 4 | 30 | 5.061 | 6.529 | 29.292 | 13.338 | 15.954 | 5.089 | 6.323 | 27.060 | 12.130 | 14.783 |
| 7 | 3 | 6 | 10 | 4.047 | 5.047 | 23.099 | 9.117 | 13.982 | 4.107 | 5.023 | 22.920 | 9.740 | 13.138 |
| 8 | 3 | 6 | 20 | 4.372 | 5.399 | 23.959 | 12.019 | 11.940 | 4.349 | 5.427 | 24.220 | 10.950 | 13.129 |
| 9 | 3 | 6 | 30 | 4.681 | 5.705 | 23.789 | 10.131 | 13.658 | 5.045 | 6.325 | 26.780 | 13.110 | 13.633 |
| 10 | 5 | 2 | 10 | 4.296 | 5.735 | 27.909 | 14.507 | 13.402 | 4.437 | 5.863 | 28.190 | 13.100 | 15.170 |
| 11 | 5 | 2 | 20 | 4.706 | 6.136 | 27.858 | 11.558 | 16.300 | 4.708 | 6.137 | 28.390 | 13.120 | 15.233 |
| 12 | 5 | 2 | 30 | 5.077 | 6.450 | 29.005 | 12.618 | 16.388 | 5.433 | 6.905 | 29.850 | 14.110 | 15.810 |
| 13 | 5 | 4 | 10 | 4.506 | 5.695 | 25.707 | 9.887 | 15.820 | 4.556 | 5.761 | 26.430 | 11.290 | 15.107 |
| 14 | 5 | 4 | 20 | 4.761 | 5.803 | 25.066 | 10.824 | 14.242 | 4.816 | 6.083 | 27.240 | 11.750 | 15.340 |
| 15 | 5 | 4 | 30 | 5.561 | 6.807 | 28.956 | 13.056 | 15.900 | 5.530 | 6.900 | 29.310 | 13.180 | 16.087 |
| 16 | 5 | 6 | 10 | 4.742 | 5.915 | 26.665 | 12.601 | 14.064 | 4.770 | 5.976 | 26.530 | 11.640 | 14.969 |
| 17 | 5 | 6 | 20 | 4.864 | 6.344 | 27.857 | 11.205 | 16.651 | 5.019 | 6.346 | 27.950 | 12.540 | 15.372 |
| 18 | 5 | 6 | 30 | 6.480 | 8.296 | 35.502 | 18.892 | 16.610 | 5.723 | 7.210 | 30.630 | 14.410 | 16.289 |
| 19 | 7 | 2 | 10 | 3.936 | 4.971 | 22.736 | 9.606 | 13.130 | 3.856 | 4.992 | 23.990 | 11.820 | 12.248 |
| 20 | 7 | 2 | 20 | 4.278 | 5.611 | 27.583 | 15.535 | 12.048 | 4.134 | 5.232 | 24.310 | 11.550 | 12.723 |
| 21 | 7 | 2 | 30 | 5.007 | 6.013 | 25.309 | 11.770 | 13.539 | 4.867 | 5.966 | 25.880 | 12.240 | 13.712 |
| 22 | 7 | 4 | 10 | 4.133 | 5.202 | 24.117 | 11.084 | 13.033 | 4.211 | 5.198 | 23.840 | 10.260 | 13.536 |
| 23 | 7 | 4 | 20 | 4.389 | 5.409 | 24.965 | 10.593 | 14.372 | 4.479 | 5.486 | 24.760 | 10.430 | 14.182 |
| 24 | 7 | 4 | 30 | 5.177 | 6.337 | 26.830 | 10.833 | 15.997 | 5.200 | 6.269 | 26.940 | 11.560 | 15.341 |
| 25 | 7 | 6 | 10 | 4.746 | 5.719 | 25.865 | 10.565 | 15.300 | 4.661 | 5.721 | 25.540 | 10.860 | 14.750 |
| 26 | 7 | 6 | 20 | 5.016 | 6.190 | 27.160 | 11.631 | 15.530 | 4.918 | 6.057 | 27.070 | 11.470 | 15.566 |
| 27 | 7 | 6 | 30 | 5.274 | 6.357 | 27.608 | 11.603 | 16.004 | 5.629 | 6.888 | 29.860 | 13.040 | 16.895 |

- The two-stage effort of obtaining a Surface Roughness (SR) model by RSM and optimization of this model, have resulted in a fairly useful method of obtaining process parameters in order to attain the improved surface quality.
- The investigation indicates that the discharge current, pulse-on time and pulse-off time are the primary factors influencing the SR of EDM8 material during EDM machining.
- Pulse-on time is found to be the dominant parameter influencing surface roughness.
- An increase in discharge current(Ip) was also observed to increase the roughness of the surface. The confirmation test showed that developed models can predict the SR accurately within 95% confidence interval.
- The methodology adopted establishes the optimization and hence facilitates the effective use of EDM machinable EN8 in industrial applications.

Results of RSM method are summarised in Table 8 for R^2 and 100-MAPE. It is observed that values are comparatively lower than that in Table 15

Table 8.: RSM method - Results of 100-MAPE and R^2

| | 100-MAPE | | | | | R^2 | | | | |
|--------------------------|----------|---------|---------|---------|---------|---------|---------|---------|---------|---------|
| | Ra | Rq | Rz | Rp | Rv | Ra | Rq | Rz | Rp | Rv |
| Surface roughness RSM | 97.2563 | 97.0520 | 96.4014 | 89.6507 | 94.9921 | 99.8075 | 99.7379 | 99.6679 | 98.1065 | 99.6734 |

4.4. Artificial Neural Network results : MSE, 100-MAPE, R^2 , using GD, GDA, LM, RP optimizers for Ra,Rq,Rz,Rp,Rv roughness characterization

4.4.1. Levenberg Marquadt (LM) - Rv

Table 9.: MSE - Training

| Model | Ra | Rq | Rz | Rp | Rv |
|--------|--------|--------|---------|--------|--------|
| 3,3,5 | 0.6145 | 0.5268 | 12.7484 | 5.7805 | 1.9906 |
| 3,4,5 | 0.2320 | 0.3116 | 5.7632 | 3.3648 | 1.5589 |
| 3,5,5 | 0.2577 | 0.3769 | 5.6313 | 4.1938 | 1.6742 |
| 3,6,5 | 0.2611 | 0.3980 | 5.8941 | 4.3860 | 1.7359 |
| 3,7,5 | 0.3598 | 0.3524 | 5.1894 | 3.7249 | 1.7618 |
| 3,8,5 | 0.4466 | 0.5745 | 9.0193 | 5.1845 | 2.2094 |
| 3,9,5 | 0.2267 | 0.4160 | 4.8924 | 3.4021 | 1.7225 |
| 3,10,5 | 0.5112 | 0.5755 | 6.4854 | 5.1552 | 2.1182 |

Table 11.: 100-MAPE - Training

| Ra | Rq | Rz | Rp | Rv |
|--------|--------|---------|---------|--------|
| 0.8816 | 0.6776 | 13.3610 | 10.9872 | 1.7374 |
| 0.2875 | 0.5838 | 11.6035 | 7.7585 | 2.7788 |
| 0.2320 | 0.4469 | 15.8244 | 7.5464 | 2.8476 |
| 0.3246 | 0.5137 | 7.2145 | 4.4629 | 2.7386 |
| 0.3732 | 0.4807 | 9.1344 | 5.6403 | 1.9395 |
| 0.4320 | 0.6740 | 10.2400 | 7.4878 | 2.7025 |
| 0.3072 | 0.4975 | 9.3864 | 5.9403 | 2.4214 |
| 0.3583 | 0.5034 | 8.1824 | 5.4917 | 2.6757 |

Table 12.: 100-MAPE-Testing

| Model | Ra | Rq | Rz | Rp | Rv |
|--------|---------|---------|---------|---------|---------|
| 3,3,5 | 89.4593 | 91.3179 | 91.4111 | 86.4767 | 92.1775 |
| 3,4,5 | 92.3164 | 93.3200 | 93.5700 | 88.9384 | 93.3983 |
| 3,5,5 | 91.9950 | 92.3777 | 94.0158 | 88.5328 | 93.2417 |
| 3,6,5 | 91.7527 | 92.0989 | 93.2501 | 88.1002 | 92.2379 |
| 3,7,5 | 90.5230 | 93.0120 | 94.3972 | 89.7952 | 92.1567 |
| 3,8,5 | 88.6511 | 90.5537 | 91.5667 | 86.1443 | 92.1446 |
| 3,9,5 | 92.6582 | 91.9939 | 94.3163 | 89.5222 | 92.6677 |
| 3,10,5 | 90.0553 | 90.5693 | 92.9260 | 87.0656 | 91.6169 |

Table 13.: R^2 - Training

| Ra | Rq | Rz | Rp | Rv |
|---------|---------|---------|---------|---------|
| 86.7293 | 89.5728 | 90.0064 | 79.0522 | 92.7297 |
| 91.4049 | 90.9243 | 90.6595 | 83.7028 | 90.0244 |
| 92.2612 | 91.4242 | 89.8107 | 84.6160 | 90.1505 |
| 90.8824 | 91.6115 | 92.6710 | 87.6929 | 90.5660 |
| 89.8605 | 91.7290 | 91.8469 | 86.2687 | 91.4846 |
| 88.2478 | 88.5413 | 89.9262 | 80.5972 | 90.4051 |
| 91.4528 | 90.9285 | 91.0559 | 85.6070 | 90.6770 |
| 90.7455 | 92.0504 | 91.6534 | 87.3093 | 90.2720 |

Table 14.: R^2 - Testing

| model | Ra | Rq | Rz | Rp | Rv |
|--------|---------|---------|---------|---------|---------|
| 3,3,5 | 97.3125 | 98.5430 | 98.2424 | 96.0009 | 99.1047 |
| 3,4,5 | 98.9802 | 99.1304 | 99.2027 | 97.7187 | 99.2958 |
| 3,5,5 | 98.8711 | 98.9524 | 99.2246 | 97.1506 | 99.2439 |
| 3,6,5 | 98.8594 | 98.8940 | 99.1891 | 97.0186 | 99.2130 |
| 3,7,5 | 98.4280 | 99.0220 | 99.2810 | 97.4483 | 99.2045 |
| 3,8,5 | 98.0326 | 98.3923 | 98.7486 | 96.4500 | 98.9990 |
| 3,9,5 | 99.0059 | 98.8388 | 99.3193 | 97.6813 | 99.2155 |
| 3,10,5 | 97.7623 | 98.4061 | 99.1010 | 96.4899 | 99.0421 |

Table

| Ra | Rq | Rz | Rp | Rv |
|---------|---------|---------|---------|---------|
| 96.1432 | 98.1774 | 98.1592 | 92.4814 | 99.2417 |
| 98.7373 | 98.3834 | 98.4129 | 94.8385 | 98.7364 |
| 99.0192 | 98.7908 | 97.8311 | 95.0236 | 98.7175 |
| 98.6094 | 98.6718 | 99.0452 | 97.1497 | 98.7152 |
| 98.4467 | 98.7549 | 98.7688 | 96.4110 | 99.1228 |
| 98.1316 | 98.1550 | 98.5770 | 94.9701 | 98.7780 |
| 98.7123 | 98.6582 | 98.7163 | 96.1578 | 98.8921 |
| 98.4620 | 98.6382 | 98.8616 | 96.5370 | 98.7453 |

Table 15.: Comparison of results of optimizers

| Optimizer | Maximum value of-(100-MAPE) | | | | | Maximum value of-R ² | | | | |
|-----------------------|-----------------------------|----------------------------|---------------------------|---------------------------|---------------------------|---------------------------------|---------------------------|---------------------------|---------------------------|---------------------------|
| | Ra | Rq | Rz | Rp | Rv | Ra | Rq | Rz | Rp | Rv |
| GD-Train Architecture | 89.6233 | 90.9756 | 95.1854 (3,4,5) | 90.1051 (3,7,5) | 92.8531 | 98.3436 | 98.5673 | 99.4371 (3,7,5) | 97.8093 (3,7,5) | 99.2045 |
| GD-Test Architecture | 89.1217 | 90.7939 | 93.5771 (3,8,5) | 88.2682 | 92.4535 | 98.2255 | 98.4715 | 99.3314 (3,7,5) | 97.1350 | 99.1621 |
| GDA-Train | 90.1563 | 91.7614 | 93.7724 | 88.5534 | 91.6212 | 98.5452 | 98.7759 | 99.2662 | 97.4794 | 99.1045 |
| GDA-Test Architecture | 90.8329 | 92.0182 | 92.8793 | 89.4264 | 91.2591 | 98.6352 | 98.8806 (3,9,5) | 99.1269 | 97.1419 | 98.9789 |
| LM-Train Architecture | 92.6582 (3,9,5) | 93.3200 (3,4,5) | 94.3972 | 89.7952 | 93.3983 (3,4,5) | 99.0059 (3,9,5) | 99.1304 (3,4,5) | 99.3193 | 97.7187 | 99.2958 (3,4,5) |
| LM-Test Architecture | 92.2612 (3,5,5) | 92.0504 (3,10,5) | 92.6710 | 86.2687 | 92.7297 (3,3,5) | 99.0192 (3,5,5) | 98.7908 | 99.0452 | 97.1497 | 99.2417 (3,3,5) |
| RP-Train | 91.7322 | 92.3465 | 94.2465 | 89.8786 | 92.0171 | 98.8003 | 98.9374 | 99.3242 | 97.7675 | 99.2058 |
| RP -Test Architecture | 90.5510 | 91.5441 | 92.5949 | 88.5802 (3,4,5) | 91.5324 | 98.3773 | 98.3773 | 99.1112 | 97.2680 (3,4,5) | 99.1168 |

5. Conclusion

It is concluded from the results that the Leven Berg-Marquardt (LM) algorithm has an accuracy using Training and testing results of MAPE and R2 is around 92% and 97% respectively for surface roughness Ra,Rq and Rv while Rz follows Gradient Descent (GD) and Root mean squared Prop (RP) follows partially GD and RP algorithms. The study proposes a deep learning-based method employing images of die-sinking EDM-machined work piece surfaces. Looking at these pictures captured by a CCD camera, the recommended method may accurately predict surface roughness values comparable to those acquired by a profilometer. With the help of this integrated technique, operators can measure roughness values that correspond to goal specifications on designs. Additionally, the learning-based technique shows promise for characterizing surface morphology and enabling automatic in-situ quality control in intelligent manufacturing cells, applicable to both EDM machining and other machining processes.

References

- [1] Anurag Joshi, Amit Kumar Saraf, and Ravi Kumar Goyal. Edm machining of die steel en8 and testing of surface roughness with varying parameters. *Materials Today: Proceedings*, 28:2557–2560, 2020.
- [2] M Mustafaiz Ahmad, R Davis, N Maurya, P Singh, and S Gupta. Optimization of process parameters in electric discharge machining process. *International Journal of Mechanical Engineering (IJME)*, 5(4):45–52, 2016.
- [3] Ushasta Aich and Simul Banerjee. Modeling of edm responses by support vector machine regression with parameters selected by particle swarm optimization. *Applied Mathematical Modelling*, 38(11-12):2800–2818, 2014.
- [4] C Balasubramaniyan, K Rajkumar, and S Santosh. Wire-edm machinability investigation on quaternary ni44ti50cu4zr2 shape memory alloy. *Materials and Manufacturing Processes*, 36(10):1161–1170, 2021.

- [5] Milan Kumar Das, Kaushik Kumar, Tapan Kumar Barman, and Prasanta Sahoo. Prediction of surface roughness in edm using response surface methodology and artificial neural network. *Journal of Manufacturing Technology Research*, 6(3/4):93, 2014.
- [6] Alessandro Giusti, Matteo Dotta, Umang Maradia, Marco Boccadoro, Luca M Gambardella, and Adriano Nasciuti. Image-based measurement of material roughness using machine learning techniques. *Procedia CIRP*, 95:377–382, 2020.
- [7] Ashish Goyal, Adithya Garimella, and Priyanka Saini. Optimization of surface roughness by design of experiment techniques during wire edm machining. *Materials Today: Proceedings*, 47:3195–3197, 2021.
- [8] C Naresh, PSC Bose, and CSP Rao. Artificial neural networks and adaptive neuro-fuzzy models for predicting wedm machining responses of nitinol alloy: Comparative study. *SN Applied Sciences*, 2:1–23, 2020.
- [9] Je-Kang Park, Bae-Keun Kwon, Jun-Hyub Park, and Dong-Joong Kang. Machine learning-based imaging system for surface defect inspection. *International Journal of Precision Engineering and Manufacturing-Green Technology*, 3:303–310, 2016.
- [10] KM Patel*, Pulak M Pandey, and P Venkateswara Rao. Determination of an optimum parametric combination using a surface roughness prediction model for edm of al₂o₃/sicw/tic ceramic composite. *Materials and Manufacturing Processes*, 24(6):675–682, 2009.
- [11] Dhiren R Patel, Vinay Vakharia, and Mysore B Kiran. Texture classification of machined surfaces using image processing and machine learning techniques. *FME Transactions*, 47(4):865–872, 2019.
- [12] Uma Maheshwera Reddy Paturi, Suryapavan Cheruku, Venkat Phani Kumar Pasunuri, Sriteja Salike, NS Reddy, and Srija Cheruku. Machine learning and statistical approach in modeling and optimization of surface roughness in wire electrical discharge machining. *Machine Learning with Applications*, 6:100099, 2021.
- [13] TR Paul, A Saha, H Majumder, V Dey, and P Dutta. Multi-objective optimization of some correlated process parameters in edm of inconel 800 using a hybrid approach. *Journal of the Brazilian Society of Mechanical Sciences and Engineering*, 41:1–11, 2019.
- [14] BC Routara, Diptikanta Das, MP Satpathy, BK Nanda, AK Sahoo, and Shubham S Singh. Investigation on machining characteristics of t6-al7075 during edm with cu tool in steady and rotary mode. *Materials Today: Proceedings*, 26:2143–2150, 2020.
- [15] Jamal Saeedi, Matteo Dotta, Andrea Galli, Adriano Nasciuti, Umang Maradia, Marco Boccadoro, Luca Maria Gambardella, and Alessandro Giusti. Measurement and inspection of electrical discharge machined steel surfaces using deep neural networks. *Machine Vision and Applications*, 32:1–15, 2021.
- [16] DM Shivanna, MB Kiran, and SD Kavitha. Evaluation of 3d surface roughness parameters of edm components using vision system. *Procedia Materials Science*, 5:2132–2141, 2014.
- [17] Ranjit Singh, Ravi Pratap Singh, and Rajeev Trehan. Machine learning algorithms based advanced optimization of edm parameters: An experimental investigation into shape memory alloys. *Sensors International*, 3:100179, 2022.
- [18] Mustafa Ulas, Osman Aydur, Turan Gurgenc, and Cihan Ozel. Surface roughness prediction of machined aluminum alloy with wire electrical discharge machining by different machine learning algorithms. *Journal of Materials Research and Technology*, 9(6):12512–12524, 2020.
- [19] Vinay Vakharia, Jay Vora, Sakshum Khanna, Rakesh Chaudhari, Milind Shah,

- Danil Yu Pimenov, Khaled Giasin, Parth Prajapati, and Szymon Wojciechowski. Experimental investigations and prediction of wedmed surface of nitinol sma using singan and densenet deep learning model. *journal of materials research and technology*, 18:325–337, 2022.
- [20] H Varol Ozkavak, MM Sofu, B Duman, and S Bacak. Estimating surface roughness for different edm processing parameters on inconel 718 using gep and ann. *cirp j manuf sci technol* 33: 306–314, 2021.
- [21] L Yogesh, M Arunadevi, and CPS Prakash. Predicton of mrr & surface roughness in wire edm machining using decision tree and naive bayes algorithm. In *2021 International Conference on Emerging Smart Computing and Informatics (ESCI)*, pages 527–532. IEEE, 2021.
- [22] Wang Zhang, Chunwang Luo, Qingyuan Ma, Zhenqiang Lin, Lan Yang, Jun Zheng, Xiaohong Ge, Wei Zhang, Yuangang Liu, and Jumei Tian. Prediction model of surface roughness of selective laser melting formed parts based on back propagation neural network. *Engineering Reports*, 5(12):e12570, 2023.
- [23] J Kundrák, I Sztankovics, and V Molnár. Accuracy and topography analysis of hard machined surfaces. *Manufacturing Technology*, 21(4):512–519, 2021.

6. Supplementary information

6.1. Declaration

- The authors have no relevant financial or non-financial interests to disclose.
- The authors have no conflicts of interest to declare that are relevant to the content of this article.
- All authors certify that they have no affiliations with or involvement in any organization or entity with any financial interest or non-financial interest in the subject matter or materials discussed in this manuscript.
- The authors have no financial or proprietary interest in the material discussed in this article.

6.1.1. Funding

The authors did not receive funding from any organization for the submitted work. Also, the authors declare they have no financial interests. Therefore, the authors have no relevant financial or non-financial interests to disclose.

6.1.2. Conflicts of interest/Competing interests

There are not any Conflicts of interest and Competing interests about the presented results in this paper. All results are based on laboratory data and based on common statistical criteria in the scientific articles. . 0

6.2. Availability of data and material

All of data and material are presented in Figures

6.2.1. Code availability

7. Annexure : I

Table 16.: ANOVA - R_v

| Source | DF | Adj SS | Adj MS | F-Value | P-Value |
|-------------------|----|---------|--------|---------|---------|
| Model | 9 | 38.4628 | 4.2736 | 4.64 | 0.004 |
| Linear | 3 | 2.4327 | 0.8109 | 0.88 | 0.472 |
| Ton | 1 | 0.3192 | 0.3192 | 0.35 | 0.564 |
| Toff | 1 | 0.1063 | 0.1063 | 0.12 | 0.739 |
| Ip | 1 | 1.9239 | 1.9239 | 2.09 | 0.168 |
| Square | 3 | 10.1324 | 3.3775 | 3.66 | 0.035 |
| Ton*Ton | 1 | 9.4514 | 9.4514 | 10.25 | 0.006 |
| Toff*Toff | 1 | 0.0732 | 0.0732 | 0.08 | 0.782 |
| Ip*Ip | 1 | 0.9629 | 0.9629 | 1.04 | 0.322 |
| 2-Way Interaction | 3 | 25.6187 | 8.5396 | 9.26 | 0.001 |
| Ton*Toff | 1 | 21.924 | 21.924 | 23.78 | 0 |
| Ton*Ip | 1 | 2.0402 | 2.0402 | 2.21 | 0.156 |
| Toff*Ip | 1 | 1.6544 | 1.6544 | 1.79 | 0.199 |
| Error | 16 | 14.7494 | 0.9218 | | |
| Total | 25 | 53.2122 | | | |

Table 17.: ANOVA - R_q

| Model | 9 | 9.9123 | 1.10136 | 7.37 | 0 |
|-------------------|----|---------|---------|-------|-------|
| Linear | 3 | 6.027 | 2.009 | 13.45 | 0 |
| Ton | 1 | 0.0009 | 0.00087 | 0.01 | 0.94 |
| Toff | 1 | 0.1961 | 0.19615 | 1.31 | 0.268 |
| Ip | 1 | 5.83 | 5.82997 | 39.04 | 0 |
| Square | 3 | 2.7048 | 0.90161 | 6.04 | 0.005 |
| Ton*Ton | 1 | 2.1877 | 2.18769 | 14.65 | 0.001 |
| Toff*Toff | 1 | 0.1501 | 0.1501 | 1.01 | 0.33 |
| Ip*Ip | 1 | 0.367 | 0.36704 | 2.46 | 0.135 |
| 2-Way Interaction | 3 | 1.1805 | 0.39349 | 2.63 | 0.083 |
| Ton*Toff | 1 | 1.139 | 1.13898 | 7.63 | 0.013 |
| Ton*Ip | 1 | 0.0137 | 0.01374 | 0.09 | 0.765 |
| Toff*Ip | 1 | 0.0277 | 0.02774 | 0.19 | 0.672 |
| Error | 17 | 2.539 | 0.14935 | | |
| Total | 26 | 12.4512 | | | |

$$\begin{aligned}
 R_v = & 19.45 + 1.48 \cdot \text{Ton} - 2.348 \cdot \text{Toff} - 0.310 \cdot \text{Ip} \\
 & - 0.331 \cdot \text{Ton}^2 + 0.0280 \cdot \text{Toff}^2 + 0.00406 \cdot \text{Ip}^2 \\
 & + 0.3379 \cdot \text{Ton} \cdot \text{Toff} + 0.0206 \cdot \text{Ton} \cdot \text{Ip} + 0.0197 \cdot \text{Toff} \cdot \text{Ip} \quad (6a) \\
 & + 0.00240 \cdot \text{Toff} \cdot \text{Ip} \quad (6b)
 \end{aligned}$$

$$\begin{aligned}
 R_q = & 4.13 + 1.239 \cdot \text{Ton} - 0.697 \cdot \text{Toff} - 0.0432 \cdot \text{Ip} \\
 & - 0.1510 \cdot \text{Ton}^2 + 0.0395 \cdot \text{Toff}^2 + 0.00247 \cdot \text{Ip}^2 \\
 & + 0.0770 \cdot \text{Ton} \cdot \text{Toff} - 0.00169 \cdot \text{Ton} \cdot \text{Ip} + 0.00240 \cdot \text{Toff} \cdot \text{Ip}
 \end{aligned}$$

Table 18.: ANOVA - Rz

| Source | DF | Adj SS | Adj MS | F-Value | P-Value |
|-------------------|----|---------|---------|---------|---------|
| Model | 9 | 113.408 | 12.6009 | 3.31 | 0.016 |
| Linear | 3 | 38.59 | 12.8633 | 3.38 | 0.043 |
| Ton | 1 | 0.56 | 0.5597 | 0.15 | 0.706 |
| Toff | 1 | 0.858 | 0.8581 | 0.23 | 0.641 |
| Ip | 1 | 37.172 | 37.1723 | 9.76 | 0.006 |
| Square | 3 | 39.498 | 13.1659 | 3.46 | 0.04 |
| Ton*Ton | 1 | 31.94 | 31.9396 | 8.38 | 0.01 |
| Toff*Toff | 1 | 5.179 | 5.1795 | 1.36 | 0.26 |
| Ip*Ip | 1 | 2.378 | 2.3785 | 0.62 | 0.44 |
| 2-Way Interaction | 3 | 35.32 | 11.7735 | 3.09 | 0.055 |
| Ton*Toff | 1 | 30.694 | 30.6944 | 8.06 | 0.011 |
| Ton*Ip | 1 | 0.157 | 0.1571 | 0.04 | 0.841 |
| Toff*Ip | 1 | 4.469 | 4.4689 | 1.17 | 0.294 |
| Error | 17 | 64.768 | 3.8099 | | |
| Total | 26 | 178.176 | | | |

$$\begin{aligned}
 R_z = & 28.07 + 3.97 \cdot \text{Ton} - 4.58 \cdot \text{Toff} - 0.259 \cdot \text{Ip} \\
 & - 0.577 \cdot \text{Ton}^2 + 0.232 \cdot \text{Toff}^2 + 0.00630 \cdot \text{Ip}^2 \\
 & + 0.400 \cdot \text{Ton} \cdot \text{Toff} + 0.0057 \cdot \text{Ton} \cdot \text{Ip} + 0.0305 \cdot \text{Toff} \cdot \text{Ip} \quad (7\text{a})
 \end{aligned}$$

$$\begin{aligned}
 R_p = & 9.80 + 3.40 \cdot \text{Ton} - 3.05 \cdot \text{Toff} - 0.113 \cdot \text{Ip} \\
 & - 0.334 \cdot \text{Ton}^2 + 0.269 \cdot \text{Toff}^2 + 0.00484 \cdot \text{Ip}^2 \quad (7\text{b}) \\
 & + 0.477 \cdot \text{Ton} \cdot \text{Toff} + 0.00484 \cdot \text{Ton} \cdot \text{Ip}
 \end{aligned}$$

Table 19.: ANOVA - Rp

| Source | DF | Adj SS | Adj MS | F-Value | P-Value |
|-------------------|----|---------|---------|---------|---------|
| Model | 9 | 40.874 | 4.5416 | 1.03 | 0.453 |
| Linear | 3 | 17.638 | 5.8793 | 1.34 | 0.295 |
| Ton | 1 | 0.003 | 0.0028 | 0 | 0.98 |
| Toff | 1 | 1.491 | 1.4907 | 0.34 | 0.568 |
| Ip | 1 | 16.144 | 16.1445 | 3.68 | 0.072 |
| Square | 3 | 19.111 | 6.3702 | 1.45 | 0.263 |
| Ton*Ton | 1 | 10.738 | 10.7379 | 2.45 | 0.136 |
| Toff*Toff | 1 | 6.967 | 6.9668 | 1.59 | 0.225 |
| Ip*Ip | 1 | 1.406 | 1.4059 | 0.32 | 0.579 |
| 2-Way Interaction | 3 | 4.126 | 1.3753 | 0.31 | 0.816 |
| Ton*Toff | 1 | 0.736 | 0.7356 | 0.17 | 0.687 |
| Ton*Ip | 1 | 1.064 | 1.0645 | 0.24 | 0.629 |
| Toff*Ip | 1 | 2.326 | 2.3258 | 0.53 | 0.477 |
| Error | 17 | 74.639 | 4.3905 | | |
| Total | 26 | 115.513 | | | |

7.0.1. Gradient Descent (GD)- Training

Table 20.: MSE

Table 21.: 100-MAPE

Table 22.: R2

| Model | Ra | Rq | Rz | Rp | Rv | Ra | Rq | Rz | Rp | Rv |
|--------|--------|--------|---------|--------|--------|---------|---------|---------|---------|---------|
| 3,3,5 | 0.7779 | 0.6526 | 8.9445 | 5.0344 | 2.6556 | 85.7883 | 90.1561 | 92.2319 | 86.7311 | 90.8281 |
| 3,4,5 | 0.4567 | 0.5673 | 4.1124 | 4.0411 | 1.7583 | 88.4859 | 90.1404 | 95.1854 | 88.8411 | 92.8531 |
| 3,5,5 | 1.1804 | 1.5216 | 8.1971 | 4.3706 | 2.7105 | 79.8802 | 83.1496 | 91.9165 | 87.6554 | 90.5394 |
| 3,6,5 | 0.6347 | 0.5138 | 5.5654 | 3.5982 | 1.8931 | 87.3674 | 90.9756 | 93.7972 | 88.8870 | 91.6324 |
| 3,7,5 | 0.5741 | 0.7259 | 4.0850 | 3.2085 | 1.8164 | 87.7135 | 89.5326 | 94.8920 | 90.1051 | 92.2929 |
| 3,8,5 | 0.5001 | 0.6199 | 5.4799 | 4.1741 | 1.5646 | 88.2882 | 89.8521 | 93.5099 | 88.2318 | 92.8523 |
| 3,9,5 | 0.3782 | 0.6075 | 5.8608 | 4.9034 | 2.2457 | 89.6233 | 90.6317 | 93.5365 | 88.3377 | 91.8186 |
| 3,10,5 | 0.6918 | 1.4944 | 10.5247 | 3.9914 | 3.1305 | 86.0773 | 82.1994 | 91.1631 | 88.4650 | 89.8138 |
| | | | | | | 96.9812 | 95.8205 | 98.5489 | 97.2733 | 98.5797 |

7.0.2. Gradient Descent (GD) - Testing

Table 23.: MSE

Table 24.: 100-MAPE

Table 25.: R2

| Model | Ra | Rq | Rz | Rp | Rv | Ra | Rq | Rz | Rp | Rv |
|--------|--------|--------|---------|--------|--------|---------|---------|---------|---------|---------|
| 3,3,5 | 0.6399 | 0.5559 | 6.8759 | 5.0609 | 3.1432 | 87.2777 | 90.7939 | 92.5721 | 86.8403 | 89.6754 |
| 3,4,5 | 0.4825 | 0.9724 | 10.4342 | 5.9997 | 3.0682 | 89.0851 | 86.3763 | 90.2636 | 85.4969 | 90.2163 |
| 3,5,5 | 1.3236 | 1.8588 | 10.7660 | 5.7609 | 4.0829 | 77.5439 | 81.2870 | 90.5205 | 85.5367 | 88.7338 |
| 3,6,5 | 0.6048 | 0.7407 | 6.2316 | 5.0843 | 1.8011 | 86.0146 | 89.1525 | 93.2920 | 86.7215 | 92.4535 |
| 3,7,5 | 0.5005 | 0.5593 | 4.9362 | 4.5105 | 2.2328 | 88.3628 | 90.2443 | 93.5032 | 87.7668 | 91.2777 |
| 3,8,5 | 0.4051 | 0.7107 | 5.2199 | 4.6831 | 3.8228 | 89.1217 | 89.0986 | 93.5771 | 86.8903 | 88.7149 |
| 3,9,5 | 0.5983 | 0.9236 | 10.9822 | 6.8305 | 3.1814 | 87.8631 | 88.3081 | 90.4847 | 85.2551 | 89.2708 |
| 3,10,5 | 0.6354 | 1.2557 | 10.8485 | 4.3429 | 4.1827 | 85.2942 | 83.2422 | 90.9524 | 88.2682 | 88.6183 |
| | | | | | | 97.1626 | 96.4773 | 98.5020 | 97.1350 | 98.1202 |

7.0.3. Gradient Descent Adaptive (GDA)- Training

Table 26.: MSE

| Model | Ra | Rq | Rz | Rp | Rv |
|--------|--------|--------|--------|--------|--------|
| 3,3,5 | 0.5686 | 1.0356 | 5.4496 | 3.6828 | 2.9641 |
| 3,4,5 | 0.5300 | 0.6708 | 5.7447 | 4.0120 | 2.2133 |
| 3,5,5 | 0.4486 | 0.6838 | 5.2934 | 4.0257 | 2.1350 |
| 3,6,5 | 1.1633 | 1.3115 | 8.3433 | 4.7127 | 1.9791 |
| 3,7,5 | 0.3687 | 0.5137 | 5.6347 | 4.1389 | 2.4303 |
| 3,8,5 | 0.3335 | 0.4533 | 6.7832 | 3.9568 | 2.4064 |
| 3,9,5 | 1.0102 | 0.5114 | 5.6333 | 4.2942 | 2.1862 |
| 3,10,5 | 0.4894 | 0.4403 | 6.0374 | 3.9208 | 2.1189 |

Table 27.: 100-MAPE

| Model | Ra | Rq | Rz | Rp | Rv |
|--------|---------|---------|---------|---------|---------|
| 3,3,5 | 86.4528 | 86.3534 | 93.2940 | 87.6888 | 90.5958 |
| 3,4,5 | 88.4843 | 89.6484 | 93.7724 | 88.5469 | 91.3603 |
| 3,5,5 | 89.0898 | 89.2792 | 93.5208 | 88.4856 | 91.6212 |
| 3,6,5 | 82.7768 | 85.3713 | 92.2289 | 88.3244 | 91.5670 |
| 3,7,5 | 89.4719 | 90.5872 | 93.3861 | 88.5534 | 91.5162 |
| 3,8,5 | 90.1563 | 91.7614 | 93.1170 | 88.3436 | 90.9095 |
| 3,9,5 | 83.0843 | 90.3237 | 93.7372 | 87.1139 | 91.2153 |
| 3,10,5 | 88.2365 | 91.4493 | 93.1689 | 88.1133 | 91.1314 |

Table 28.: R2

| Model | Ra | Rq | Rz | Rp | Rv |
|--------|---------|---------|---------|---------|---------|
| 3,3,5 | 97.5037 | 97.1537 | 99.2447 | 97.4794 | 98.6623 |
| 3,4,5 | 97.6690 | 98.1332 | 99.2069 | 97.2765 | 98.9994 |
| 3,5,5 | 98.0527 | 98.0915 | 99.2662 | 97.2544 | 99.0316 |
| 3,6,5 | 94.9193 | 96.3785 | 98.8523 | 96.7933 | 99.1045 |
| 3,7,5 | 98.3734 | 98.5749 | 99.2184 | 97.1670 | 98.8995 |
| 3,8,5 | 98.5452 | 98.7442 | 99.0651 | 97.3328 | 98.9120 |
| 3,9,5 | 95.6234 | 98.5791 | 99.2248 | 97.0784 | 99.0133 |
| 3,10,5 | 97.8545 | 98.7759 | 99.1642 | 97.3340 | 99.0411 |

7.0.4. Gradient Descent Adaptive(GDA) - Testing

Table 29.: MSE

| Model | Ra | Rq | Rz | Rp | Rv |
|--------|---------|---------|---------|---------|---------|
| 3,3,5 | 86.2255 | 81.3561 | 91.5968 | 83.2096 | 86.5399 |
| 3,4,5 | 89.8145 | 90.1799 | 92.7173 | 87.7070 | 90.4629 |
| 3,5,5 | 88.2345 | 89.9694 | 91.7693 | 84.2450 | 89.9527 |
| 3,6,5 | 80.6744 | 84.2998 | 88.5244 | 89.4264 | 90.6904 |
| 3,7,5 | 89.8009 | 89.8489 | 92.8793 | 88.5134 | 90.8829 |
| 3,8,5 | 90.3000 | 91.7128 | 92.6720 | 86.7530 | 89.8871 |
| 3,9,5 | 84.9822 | 92.0182 | 91.6488 | 86.1571 | 91.2591 |
| 3,10,5 | 90.8329 | 89.7613 | 91.4751 | 83.8114 | 90.9820 |

Table 30.: 100-MAPE

| Model | Ra | Rq | Rz | Rp | Rv |
|--------|---------|---------|---------|---------|---------|
| 3,3,5 | 96.8157 | 94.3810 | 98.6514 | 95.4307 | 97.7344 |
| 3,4,5 | 97.6310 | 98.2550 | 98.9794 | 97.1302 | 98.7297 |
| 3,5,5 | 97.9157 | 98.0614 | 98.7519 | 95.5996 | 98.6494 |
| 3,6,5 | 93.7295 | 96.0410 | 97.7044 | 96.9431 | 98.9789 |
| 3,7,5 | 98.6352 | 98.2254 | 99.0462 | 97.1419 | 98.8271 |
| 3,8,5 | 98.5637 | 98.7345 | 99.1269 | 97.0021 | 98.7903 |
| 3,9,5 | 96.5746 | 98.8806 | 98.8405 | 97.0004 | 98.9480 |
| 3,10,5 | 98.6296 | 98.3069 | 98.8783 | 95.8303 | 98.9596 |

Table 31.: R2

7.0.5. Root Mean Square Prop (RP)- Training

Table 32.: MSE

| Model | Ra | Rq | Rz | Rp | Rv |
|--------|--------|--------|--------|--------|---------|
| 3,3,5 | 0.4054 | 0.4503 | 3.4458 | 2.4101 | 90.1411 |
| 3,4,5 | 0.2750 | 0.3780 | 5.1033 | 3.2810 | 2.0257 |
| 3,5,5 | 0.7747 | 0.5886 | 6.3194 | 5.7125 | 2.9942 |
| 3,6,5 | 0.4220 | 0.5742 | 6.0855 | 4.4157 | 2.7196 |
| 3,7,5 | 0.3055 | 0.5751 | 5.0551 | 4.1009 | 1.7572 |
| 3,8,5 | 0.3493 | 0.6995 | 5.9264 | 4.7299 | 2.1577 |
| 3,9,5 | 0.4623 | 0.5240 | 5.6926 | 4.4099 | 2.1416 |
| 3,10,5 | 0.3602 | 0.7306 | 6.6492 | 4.3102 | 2.2201 |

7.0.6. Root Mean Square Prop (RP) - Testing

Table 35.: MSE

| Model | Ra | Rq | Rz | Rp | Rv |
|--------|--------|--------|---------|---------|--------|
| 3,3,5 | 0.4737 | 0.5547 | 12.3075 | 11.5809 | 3.0096 |
| 3,4,5 | 0.3868 | 0.4548 | 7.2609 | 4.3790 | 2.6160 |
| 3,5,5 | 0.5372 | 0.5277 | 8.1677 | 5.5556 | 3.1009 |
| 3,6,5 | 0.4813 | 0.7669 | 9.5201 | 5.7815 | 2.9498 |
| 3,7,5 | 0.3966 | 0.6212 | 6.6503 | 4.4882 | 1.9346 |
| 3,8,5 | 0.4811 | 0.9717 | 8.2418 | 5.6460 | 2.1646 |
| 3,9,5 | 0.4332 | 0.4443 | 6.5408 | 5.8276 | 2.1740 |
| 3,10,5 | 0.3805 | 0.5641 | 7.6993 | 4.3662 | 2.1690 |

Table 33.: 100-MAPE

Table 34.: R2

| Model | Ra | Rq | Rz | Rp | Rv |
|--------|---------|---------|---------|---------|---------|
| 3,3,5 | 90.1411 | 91.5349 | 93.9577 | 88.3675 | 91.1815 |
| 3,4,5 | 91.7322 | 92.3465 | 93.5874 | 89.8786 | 91.7955 |
| 3,5,5 | 86.4465 | 91.2328 | 93.2535 | 86.3609 | 90.4673 |
| 3,6,5 | 89.4115 | 90.0583 | 93.1604 | 87.3306 | 90.8630 |
| 3,7,5 | 91.0168 | 91.1963 | 94.2465 | 88.3646 | 92.0171 |
| 3,8,5 | 90.8580 | 89.0613 | 93.2316 | 87.5726 | 91.7430 |
| 3,9,5 | 88.3711 | 91.0014 | 93.1476 | 86.2296 | 91.1224 |
| 3,10,5 | 90.0833 | 89.3810 | 92.8481 | 87.2978 | 91.2643 |

Table 35.: 100-MAPE

Table 36.: R2

| Model | Ra | Rq | Rz | Rp | Rv |
|--------|---------|---------|---------|---------|---------|
| 3,3,5 | 98.2355 | 98.7381 | 99.3242 | 97.6505 | 98.9130 |
| 3,4,5 | 98.8003 | 98.9374 | 99.2944 | 97.7675 | 99.0806 |
| 3,5,5 | 96.6567 | 98.3798 | 99.1325 | 96.1491 | 98.6486 |
| 3,6,5 | 98.1402 | 98.3985 | 99.1562 | 96.9706 | 98.7686 |
| 3,7,5 | 98.6655 | 98.4001 | 99.3009 | 97.2014 | 99.2058 |
| 3,8,5 | 98.4601 | 98.0393 | 99.1799 | 96.7704 | 99.0225 |
| 3,9,5 | 97.9749 | 98.5410 | 99.2138 | 96.9953 | 99.0321 |
| 3,10,5 | 98.4134 | 97.9456 | 99.0786 | 97.0486 | 98.9952 |